Homogeneous nucleation: theory and experiment

J. Phys.: Condens. Matter 4 (1992) 7627–7650. Printed in the UK

REVIEW ARTICLE

Homogeneous nucleation: theory and experiment

David W Oxtoby

James Franck Institute and Department of Chemistry, University of Chicago, 5640 S Ellis Avenue, Chicago, IL 60637, USA

Received 13 July 1992

Abstract. Recent theoretical and experimental advances in the study of homogeneous nucleation are reviewed, with emphasis placed on phase transitions involving single-component liquids (condensation, cavitation, and crystallization from the melt). Extensions of classical nucleation theory are described and compared with new experiments that now directly measure nucleation rates. Novel methods of statistical mechanics, including density-functional theory and computer simulations, are presented. The recent rapid evolution of this field has opened up many new questions for further research.

1. Introduction

In a first-order phase transition, there is a discontinuous change in some order parameter between the two phases. Such a change is driven by lowering of the free energy as the new phase forms. Close to the equilibrium transition point, the original phase remains metastable, however, and a fluctuation is required to cause the appearance of the first region of the new phase. Such a process of nucleation is thermally achieved and, depending on the height of the free-energy barrier, its rate can be very slow or very fast. In the former case, large deviations from equilibrium may be required before the stable phase first appears, and significant hysteresis will be seen across the transition.

Nucleation has many practical consequences in science and technology. In materials science, the casting of metals gives physical properties that depend on the conditions of crystal growth. If large undercoolings can be achieved before nucleation occurs (as in rapid solidification processing [1]) different and potentially useful forms of the metals may be produced. In atmospheric sciences, the nucleation of both water droplets and ice crystals in the atmosphere has a major effect both short-term on the weather and long-term through global warming (or cooling) by cloud formation caused by atmospheric aerosols [2]. In biology, there is much interest in bypassing nucleation of ice in the cryopreservation of human tissues [3].

Although nucleation potentially plays a role in the dynamics of every first-order transition, this review will be limited to a number of fundamental aspects. It will consider only single-component systems, and thus leave out some very interesting aspects of condensation of binary vapours or crystallization of alloys. It will discuss only homogeneous nucleation, that occuring in the bulk of a pure phase, and thus ignore the important practical subject of heterogeneous nucleation by impurities

0953-8984/92/387627+24$04.50

or on surfaces. Finally, the emphasis will be on nucleation involving liquids: the condensation of liquids from the vapour (the most thoroughly studied case), the cavitation or bubble formation that results when a liquid is placed under negative pressure, and the crystallization of solid from the melt (the reverse process of melting of a solid generally occurs at the surface or near grain boundaries, and is rarely homogeneous). In all of these areas there have been recent important advances, involving a combination of more accurate experiments, new theoretical methods, and novel computer simulations.

Section 2 outlines a general theory of nucleation, stressing what approximations are made at each stage. Although this section is based on earlier work [4], the actual approach presented is new, and avoids some of the problems of other methods that depend on quasi-equilibrium descriptions of what is certainly a non-equilibrium process. This section concludes with a description of traditional classical nucleation theory. Section 3 introduces some of the new experimental techniques for studying both gas–liquid and liquid–solid nucleation, without providing an exhaustive list of all recent experiments. Section 4 describes some modifications of classical nucleation theory, while section 5 introduces a new statistical mechanical approach based on density-functional theory. Finally, section 6 summarizes some recent computer simulations that bear on the interpretation of nucleation experiments.

Two earlier reviews on nucleation by the present author have had somewhat different emphases: [5] concerned only liquid–solid nucleation, and [6] was primarily oriented toward density-functional methods. Although both of these subjects are discussed in this article, the purpose here is to present a broader overview of recent advances.

2. Steady-state nucleation

2.1. Nucleation kinetics

A theory of nucleation must have at its centre a model for the rates and mechanisms by which small clusters of the new phase gain or lose particles. Even before this can be attempted, however, it is necessary to identify the nucleus itself. For condensation from a low-density gas, or for crystallization from dilute solution, it is straightforward to identify isolated large clusters, as they differ sharply in density or composition from their immediate surroundings. It is much less evident how to draw boundaries in fluids near the critical point, however, or in a crystal forming from the melt. In these cases, the very identification of a number of particles i with a nucleus at a given time can be problematical, and continuum methods such as those discussed in section 5 may be more appropriate.

Suppose, however, that we restrict ourselves to the simpler cases in which a molecule number can be assigned to a nucleus. Nucleation dynamics then involves a set of rate equations by which clusters of different sizes gain or lose particles. Note first that the very act of writing time-local rate equations involves an assumption about lack of memory: the probability that a given cluster will undergo a particular change in particle number during a time interval is independent of its past history. In other words, there is not correlation between successive events that change particle number in a cluster. Moreover, the use of rate constants involves the implicit assumption that the temperature does not change as clusters grow or shrink. As the phase change must entail the evolution of heat, this means that clusters are thermally

equilibrated between collisions that change particle number. In some gas–liquid nucleation experiments, this is achieved by working with a large excess of an inert background gas such as helium. Little work has been done for the situation where this not true and temperature changes result [7].

The next assumption that is usually made is that clusters grow or shrink via the attachment or loss of single molecules. Events in which pre-existing clusters collide and fuse are ignored, as are those in which a cluster fissions into two or more other clusters. This should be a reasonable approximation for condensation at low pressures, where almost all molecules are isolated 'monomer', but it does not appear to have been tested in any extensive way. Making this approximation leads to a set of coupled rate equations for the number densities $n(i,\ t)$ of clusters of size i at time t. They have the form

$$\partial n(i,\ t)/\partial t = \beta(i-1)n(i-1,\ t) - \gamma(i)n(i,\ t) - \beta(i)n(i,\ t) + \gamma(i+1)n(i+1,\ t) \tag{1}$$

where $\beta(i)$ is the forward rate at which a cluster of size i gains particles, and $\gamma(i)$ is the backward rate at which it loses particles. The forward rate will depend on the concentration of single molecules in the surroundings, and in the simplest case will be proportional to that concentration. If monomer depletion is significant over the time-scale studied, then of course this forward rate constant will change with time.

Equation (1) provides a starting point for studies of transient nucleation. Given an initial distribution of clusters of size i (or perhaps no clusters at all, only monomer) how does the cluster distribution evolve with time after an abrupt change in temperature or pressure? It is usually the case that after a transient time τ during which the cluster distribution changes, a steady state emerges in which there is a continuous flux of monomer coverted to large clusters, but the distribution of intermediate-size clusters stops changing. The nature of this transient nucleation (and the calculation of the transient time τ) has attracted recent interest [8–13]. Transient nucleation can be studied experimentally by counting crystallites as a function of time in liquids near their glass transition [14, 15], and programmed quenches (in which the sample is held for a period at two or more tempertures) can be used to gain still more information about transient nucleation kinetics [16, 17]. These areas lie outside the scope of this review, however, and are not considered further here.

Define a flux $J(i+\frac{1}{2})$ as the net rate at which clusters of size i become clusters of size $i+1$. It is given by [4]

$$J(i+\tfrac{1}{2},\ t) = \beta(i)n(i,\ t) - \gamma(i+1)n(i+1,\ t) \tag{2}$$

so that

$$\partial n(i,\ t)/\partial t = J(i-\tfrac{1}{2},\ t) - J(i+\tfrac{1}{2},\ t). \tag{3}$$

Let us now consider a steady state, in which the populations of different sizes of clusters no longer depend on time. In some experiments (see section 3) this is achieved by removing large enough clusters and breaking them up into monomer again; in other cases the steady state is a plateau region that is reached after a characteristic transient time destroys initial conditions but before significant monomer depletion occurs. In the steady state, all fluxes are equal to a single constant flux J:

$$J(i+\tfrac{1}{2},\ t) = J \qquad (\text{all } i,\ t) \tag{4}$$

and it is this flux that is identified with the nucleation rate sought by theory or experiment.

To proceed further, it is convenient to define a function $f(i)$ by the recursion relation

$$f(i+1) = [\beta(i)/\gamma(i+1)]f(i) \tag{5}$$

with $f(1) = 1$. Dividing (2) by $\beta(i)f(i) = \gamma(i+1)f(i+1)$ (after setting J to a constant in the steady state) gives

$$J/\beta(i)f(i) = n(i)/f(i) - n(i+1)/f(i+1). \tag{6}$$

This equation can be summed from $i = 1$ to a limiting value $i = i_{max}$, giving

$$J\sum_{i=1}^{i_{max}} \frac{1}{\beta(i)f(i)} = n(1) - \frac{n(i_{max})}{f(i_{max})}. \tag{7}$$

Let us now examine the dependence of $f(i)$ on i. This function can be rewritten as

$$f(i) = \prod_{j=1}^{i-1} \frac{\beta(j)}{\gamma(j+1)}. \tag{8}$$

The ratio $\beta(i-1)/\gamma(i)$ is the rate at which a cluster of size $i-1$ gains a particle divided by the reverse rate at which the cluster of size i loses a particle. Exactly at phase coexistence, in the thermodynamic limit of large enough i, these rates are equal. In the metastable state studied in nucleation experiments, however, the new phase is thermodynamically stable, and this means that for large enough i this ratio must be larger than 1 (the forward rate must be larger than the reverse). For large i, then, $f(i)$ must grow with i, increasing by a factor larger than 1 for each increase in i by 1. (This in fact corresponds to exponential growth of f with i.) We must clearly have $n(i_{max}) < n(1)$ (as otherwise the assumption of little depletion of monomer would be drastically violated). By choosing i_{max} large enough, the second term on the right side of (7) will then be negligible compared to the first. Because $\beta(i)$ is a smooth and (at least for large i) increasing function of i, the sum on the left side of this equation can be extended to infinity, with convergence guaranteed by the exponential fall-off of $1/f(i)$. This leaves

$$J = n(1)\left(\sum_{i=1}^{\infty} \frac{1}{\beta(i)f(i)}\right)^{-1}. \tag{9}$$

This equation gives a direct expression for the nucleation rate in terms of the forward and reverse rate constants.

2.2. *Classical nucleation theory*

Up to this point, the approximations introduced have been well controlled. The next step is straightforward for condensation from dilute gases (or crystallization from

dilute solution) but less evident for crystallization from the melt or for cavitation. The latter cases will be considered further in section 2.3.

The forward rate constant for addition of a particle to a cluster in a dilute gas should be proportional to the gas pressure, so that $\beta(i)$ can be written [4] as $S\beta_e(i)$, where $S = P/P_e$ is the supersaturation, the ratio of the actual pressure to the equilibrium vapour pressure of the liquid at the same temperature T, and $\beta_e(i)$ is the forward rate constant at pressure P_e. The rate at which a cluster loses particles (the reverse rate constant), on the other hand, should be independent of gas pressure so that $\gamma(i) = \gamma_e(i)$. The function $f(i)$ then has the form

$$f(i) = S^{i-1} \prod_{j=1}^{i-1} \frac{\beta_e(j)}{\gamma_e(j+1)}. \tag{10}$$

The ratio of products of rate constants in (10) has a simple interpretation: it is the equilibrium constant for the formation of a cluster of size i from isolated molecules, all at pressure P_e. This implies that

$$f(i) = S^{i-1} \exp(-\Delta G_i / k_B T) \tag{11}$$

where ΔG_i is the Gibbs free energy change for the reaction

$$iA \leftrightarrow A_i \tag{12}$$

and k_B is the Boltzmann constant. For condensation from solution, the analogous relations involving supersaturation of the solute particles are evident. The result is an expression for nucleation rates in terms of equilibrium free-energy changes for cluster formation.

Classical nucleation theory then makes a single rather drastic approximation. Suppose the i molecules are converted to a cluster by the following pathway: first the molecules are transferred from the gas phase (at pressure P_e) to the liquid phase at the same pressure. The free-energy change for this step is zero, because the two phases coexist at this pressure. Then a droplet of size i is 'carved out' of the liquid and separated from it. The latter step involves the creation of additional interface between gas and liquid, so a reasonable approximation for the free-energy change is

$$\Delta G_i = \sigma A(i) \tag{13}$$

where σ is the surface tension of the gas–liquid interface and $A(i)$ is the surface area of a cluster of size i. If the cluster is taken to be spherical and to have the same volume per particle v_l as the bulk liquid, then

$$A(i) = (36\pi)^{1/3} v_l^{2/3} i^{2/3}. \tag{14}$$

Classical nucleation theory thus relies on a macroscopic approximation for the free energy of clusters. It obviously makes no sense for small clusters of a few molecules, but (as we shall see) this does not matter. Whether it is correct for clusters of, let us say, 100 molecules is a separate question that must be tested against experiment or against carefully controlled theoretical calculations. Let us define a reduced (dimensionless) surface tension through [18]

$$\theta = (36\pi)^{1/3} v_l^{2/3} \sigma / k_B T. \tag{15}$$

The nucleation rate then has the form (combining (9), (11) and (13))

$$J = n(1)\left(\sum_{i=1}^{\infty} \frac{1}{\beta_e(i)S^i \exp(-\theta i^{2/3})}\right)^{-1}. \tag{16}$$

Examine the three terms in the denominator of the sum in (16). The first is $\beta_e(i)$ and varies relatively slowly with i (for a spherical nucleus it will grow as the $\frac{2}{3}$ power of i). The second term grows exponentially with i (because $S > 1$), while the third term falls off exponentially with $i^{2/3}$. The combination of these last two terms means that the denominator initially decreases rapidly as i increases from 1, it then reaches a minimum, and finally increases as the S^i term begins to dominate. The terms in the sum, then, are largest near the minimum in the denominator. Setting the derivative of the denominator to zero at its minimum then defines the size of the critical nucleus i^* via the equation

$$(\mathrm{d}/\mathrm{d}i)\left(\beta_e(i)S^i \exp(-\theta i^{2/3})\right) = 0 \qquad \text{at } i = i^*. \tag{17}$$

In practice, $\beta_e(i)$ is usually taken to vary slowly with i and is removed from the sum and replaced by $\beta_e(i^*)$. The two exponential terms can be written as $\exp(-g(i))$, where $g(i) = \theta i^{2/3} - i \ln S$. Setting the derivative of $g(i)$ to zero then gives

$$i^* = \left(\frac{2\theta}{3 \ln S}\right)^3 = \frac{32\pi}{3}\frac{v_l^2\sigma^3}{(k_BT)^3(\ln S)^3}. \tag{18}$$

If the critical nucleus i^* is large enough, then many terms near i^* contribute to the sum and it can be replaced by an integral. In the method of steepest descents, the function $\exp(g(i))$ is approximated near its maximum by

$$\exp(g(i)) \approx \exp(g(i^*)) \exp\left(-\tfrac{1}{2}|g''(i^*)|(i - i^*)^2\right) \tag{19}$$

where $g''(i)$ is the second derivative of $g(i)$ and the integration is extended to $\pm\infty$. Taking $g(i)$ as above then gives the final result for the steady-state rate:

$$J = (n(1)\beta_e(i^*)/3)(\theta/\pi)^{1/2}(i^*)^{-2/3} \exp\left[-\tfrac{4}{27}\theta^3/(\ln S)^3\right]. \tag{20}$$

It should be stressed that the approximation leading from (16) to (20) are mathematical, not physical ones. The actual result of classical nucleation theory is embodied in (16), which can easily be evaluated by numerical summation.

To complete the theory, the forward rate $\beta_e(i)$ must be evaluated in the vicinity of the critical nucleus size i^*. If the nucleus is taken to be spherical (as above) and collisions of monomer with its surface are taken to occur at the gas kinetic rate for an ideal gas, then

$$\beta_e(i) = (k_BT/2\pi m_1)^{1/2}(n(1)/S)A(i) \tag{21}$$

where m_1 is the mass of monomer molecules and the surface area of the cluster $A(i)$ is defined in (14). We have also used the fact that the monomer concentration at pressure P_e is reduced from its value $n(1)$ at the pressure of the nucleation

experiment by a factor of S. Inserting this into (20) gives the final result from classical nucleation theory for condensation from a dilute vapour:

$$J = \left(\frac{2\sigma}{\pi m_l}\right)^{1/2} \frac{v_l n(1)^2}{S} \exp\left(-\frac{16\pi}{3} \frac{v_l^2 \sigma^3}{(k_B T)^3 (\ln S)^2}\right). \tag{22}$$

The equivalent result for crystallization from a dilute solution can easily be calculated by using the rate at which solute particles diffuse to the surface of the growing nucleus for $\beta_e(i^*)$.

Equation (22) differs in two respects from other often quoted predictions [19]. First, other approaches sometimes introduce a multiplicative factor (less than 1) which is the sticking probability of a molecule colliding with a liquid surface. This factor is assumed here to be unity. Second, the factor of S in the denominator of (22) is often omitted. It results from a correct treatment of the nucleation kinetics, and its presence was first pointed out by Courtney in 1961 [20]. Blander and Katz reached a similar conclusion independently in 1972 [21]. Many comparisons of 'classical nucleation theory' with experiment have omitted this factor; in the future it would be more correct to include it.

2.3. Crystallization from the melt and cavitation

The theory presented in sections 2.1 and 2.2 was designed to predict the nucleation rate for condensation from a dilute vapour or crystallization from a dilute solution. In this section, some of the difficulties with extending that theory to other types of nucleation processes are pointed out.

It has already been stated that it may not be easy to identify nuclei in the case of crystallization from the melt. One promising approach is to examine the local coordination about atoms, which differs between liquid and crystal, and to use that to identify clusters [22]. Even if this can be done, however, there are problems with applying the approach described earlier in this section to crystallization. For example, the kinetic approach of section 2.1 took advantage of the very reasonable assumptions that the forward rate is proportional to gas density while the reverse rate is independent of gas density. This allowed the nucleation rates to be rewritten in terms of free-energy changes for clusters in stable equilibrium at pressure P_e. Such simplifying approximations are not possible for crystallization from the melt. Although Katz and Spaepen [23] have extended the kinetic approach to condensed systems, they were forced to use negative pressures to stabilize clusters at fixed temperature, and to make *ad hoc* assumptions about the variation of rates with pressure.

If the full kinetic approach is abandoned, it is still possible to obtain nucleation rates in the form

$$J = J_0 \exp(-\Delta G^*/k_B T) \tag{23}$$

where ΔG^* is now the free energy of formation of the critical crystallization nucleus in unstable equilibrium with the fluid. Classical nucleation theory takes

$$\Delta G(i) = -i\,\Delta\mu_{sl} + \sigma_{sl} A(i) \tag{24}$$

where σ_{sl} is the solid–liquid surface free energy and $\Delta\mu_{sl}$ is the difference in chemical potential (Gibbs free energy per particle) between bulk liquid and bulk solid. The latter is given by

$$\Delta\mu_{sl} = \Delta h_{sl}(T) - T\,\Delta s_{sl}(T) \tag{25}$$

where Δh and Δs are the (temperature-dependent) enthalpy change and entropy change per particle in the solid–liquid transition. If these are approximated as independent of temperature, then

$$\Delta\mu_{sl} \simeq \Delta h_{sl}((T_f - T)/T_f) \tag{26}$$

where T_f is the equilibrium freezing temperature. (Alternatively, if heat capacities can be measured or estimated for crystal and undercooled liquid, a more accurate temperature dependence can be used.) The undercooling $T_f - T$ then provides the driving force for nucleation. Inserting (26) into (24) and finding the maximum ΔG^*, assuming the critical nucleus to be spherical, gives

$$J = J_0 \exp\left(-\frac{16\pi}{3}\frac{v_s^2\sigma_{sl}^3}{k_B T(\Delta h_{sl})^2(1 - T/T_f)^2}\right) \tag{27}$$

which is a straightforward generalization of (22).

Two important questions arise concerning (27). The first is whether σ_{sl} should be assigned its value at T_f, or if some correction should be made for the fact that the actual temperature T may be substantially below T_f. This is a difficult problem, especially because the only place a surface free energy can be measured (even in principle) is under conditions where the two phases coexist, namely at T_f. Thus, solid–liquid nucleation raises not only the question of whether the surface free energy is size dependent (as in gas–liquid nucleation) but also whether it is temperature dependent. The second question about (27) concerns the pre-exponential factor J_0. Not only is there no kinetic approach to estimate this factor (as in section 2.2) but it is also unclear what value should be assigned to the forward rate $\beta(i^*)$. Early work on liquid–solid nucleation assumed that atoms or molecules in the melt diffused until they 'jumped' across the liquid–solid interface, giving as a pre-exponential factor the rate of diffusion across a distance of the order of interparticle separations in the liquid [24]. It is not evident, however, that diffusion is relevant in a pure liquid, or whether the characteristic rate for the elementary process should simply be a phonon frequency. It is also quite possible that the proper description of dynamics should involve collective modes, in which fluctuations in local structure lead to the sudden appearance of crystalline regions with many particles, rather than the stepwise growth process useful for gas–liquid nucleation.

Similar questions arise in the calculation of rates of bubble nucleation (cavitation). Within the context of classical nucleation theory, it is possible to estimate the free energy to create a spherical cavity in a liquid under tension. As the radius of this cavity increases, its free energy should first increase (because of surface tension) and then decrease (because the vapour phase is more stable than the liquid in bulk). The critical bubble size can be defined, and its free energy estimated from classical nucleation theory. The pre-exponential factor is quite difficult to estimate, however. What is the 'population' of elementary 'cavities' in the liquid, which provides the analogue of the $n(1)$ term for gas–liquid nucleation? What are the rates of the dynamic processes by which these cavities coalesce to form the critical droplet?

There are many open questions concerning nucleation kinetics of crystals and vapour bubbles from the liquid phase.

3. Experimental measurements of nucleation rates

3.1. Gas–liquid nucleation

The traditional method of studying gas–liquid nucleation involves the use of a cloud chamber. At a given temperature, the supersaturation of the vapour S is adjusted until droplet formation is observable. Because droplet growth beyond the critical nucleus is fast, the rate at which macroscopic droplets appear is close to the rate of formation of critical nuclei. The nucleation rate changes so rapidly with supersaturation that it is very small (almost unobservable) for supersaturations smaller than a critical supersaturation S_c and very large for larger values of S. This allows an approximate determination not of the actual rate, but of the value of S where J passes through a magnitude of order 1. The critical supersaturation S_c can then be compared with the prediction of classical nucleation theory. The results are generally good: classical theory predicts values of S_c that are typically accurate to within 10% for most substances [25]. It should be stressed, however, that a variation of 10% in S leads to changes in J by many orders of magnitude.

There are at least three cases in which classical nucleation theory gives predicted supersaturations in strong disagreement with experiment. The first is the condensation of styrene from the vapour, where the measured S_c is much smaller than predicted [26]. Reiss and co-workers have investigated this system and have argued persuasively that gas-phase polymerization occurs in styrene. The resulting short polymers (oligomers) then provide sites for the subsequent heterogeneous nucleation of liquid droplets of styrene monomer. The method appears to be extremely sensitive to oligomer length, and provides a promising way to study gas-phase polymerization [27].

Experimental critical supersaturations for acetonitrile, on the other hand, are significantly higher than predicted [28]. El-Shall has argued that the alignment of dipoles near the surface of nuclei (in comparison with that at a planar interface) can help to explain this discrepancy. A quantitative theory is not available, however, nor is it clear why no large deviations from classical theory are found in other dipolar liquids such as water, for example.

A third area where substantial deviations from classical theory are seen is in the condensation of liquid metals such as mercury from the vapour. Here, measured values of S_c can be as much as three orders of magnitude smaller than predicted by classical theory [29]. A reasonable explanation for these extremely large effects is that small clusters of mercury atoms are insulators, with much smaller effective surface tensions than those measured for bulk metallic mercury. A downward adjustment of the surface tension by about 40% is sufficient to account for the observations.

In recent years, new experimental techniques have been developed to measure actual rates, instead of just critical supersaturations, and thus to provide a more stringent test of classical nucleation theory. One method used is the upward thermal diffusion cloud chamber of Katz and co-workers [30, 31]. In this device, a temperature gradient is established between a warm pool of fluid on the bottom and a cooler upper surface. This gives rise to a supersaturation that has a maximum value at some height in the container. The two temperatures are adjusted so that the nucleation rate at this location is measurable (it is typically in the range 10^{-4} to 10 cm^{-3} s^{-1}. By using thermodynamic and transport properties of the gas, the supersaturation and temperature at the height where nuclei form can be calculated, and the results compared with theory.

A second technique uses a fast-expansion piston cloud chamber. In this, a gas is abruptly compressed to a supersaturated state and held for a short interval (a fraction of a second, typically). Nuclei form during this interval, after which the piston is pulled back to give a vapour that is still sufficiently supersaturated for the existing nuclei to grow to observable size, but not such that additional nuclei form. The total number of droplets formed is then counted. This technique has the advantage of being spatially homogeneous (in comparison to the thermal diffusion cloud chamber), but it is temporally inhomogeneous. The time to establish a steady state must be significantly shorter than the period during which the system is held at its highest supersaturation. This method has been applied by Schmitt and co-workers [32, 33] to study nucleation rates from 10^2 to 10^5 cm^{-3} s^{-1} and by Wagner and Strey [34, 35] to study rates of 10^6 to 10^{10} cm^{-3} s^{-1}. A variant of this method using a shock tube has been described by Peters and Paikert [36].

The different techniques just described access rates that vary over 14 orders of magnitude. Nonane, C_9H_{20}, has been studied by three research groups and consistent results have been observed [31, 33, 34]. Other studies have focussed on water [37], toluene [32], and the *n*-alcohols [35, 36]. The consensus of this work is that the variation of nucleation rate with supersaturation predicted by classical theory

$$\ln J \approx A(T) - B(T)/(\ln S)^2 \tag{28}$$

is approximately correct, but that the temperature dependence is not. Predicted nucleation rates are typically too low at low temperature, and too high at high temperature, with errors on the order of several orders of magnitude in either direction. These results have stimulated the search for improved theories of nucleation, some of which we shall consider in sections 4 and 5.

3.2. Liquid–solid nucleation

Nucleation of the liquid–solid transition involves additional assumptions that make the interpretation of such experiments more problematical than in the case of gas–liquid nucleation. The first difference relates to the surface free energy σ_{sl}. The analogous quantity for the gas–liquid transition, the surface tension, is easily measurable to high accuracy. The liquid–solid surface free energy, on the other hand, has only been measured in certain special cases [5]. Moreover, as pointed out in section 2.3, these experiments are typically at temperatures that may differ by hundreds of degrees from the nucleation conditions. As a result, measurements of nucleation rates for crystallization from the melt cannot provide stringent tests of classical theory.

A second problem with nucleation experiments involving liquids (cavitation as well as crystallization) is an even more fundamental one: it is difficult to purify a liquid to exclude impurities than can catalyze nucleation. Liquid–solid nucleation is almost always heterogeneous except in special situations. There are two ways to limit the role of impurity nucleation. One is to divide the sample into tiny enough portions that many of these will not contain a heterogeneous nucleation site. A second is to work under conditions where the nucleation rate is high enough (and the growth rate low enough) that most of the nuclei form homogeneously. The first method has been applied to crystallization of liquid metals and to aqueous salt solutions, and the second to nucleation in silicate melts near their glass transition.

Turnbull pioneered the study of nucleation in liquid metals by devising a technique in which a liquid metal sample was broken up into an emulsion of tiny droplets

suspended in oil [38]. As such a suspension is cooled, its state is monitored by measuring a physical property such as the volume or the heat of crystallization evolved as the droplets undergo phase changes. Some droplets crystallize at temperatures slightly below T_f because they contain active nucleation catalysts. The others remain liquid until a definite temperature T_n is reached, at which point all crystallize. This nucleation temperature is sharply defined because, as (27) shows, the nucleation rate changes from being extremely fast to extremely slow over a very small temperature range. Turnbull associated T_n with the homogeneous nucleation temperature of the liquid metal, and used classical nucleation theory to estimate the liquid–solid surface free energy. Typical values for T_n were 20–35% lower than T_f.

Subsequent work by Perepezko, however, revealed that the limiting temperature T_n could in some cases be lowered further by using a different oil medium [39]. This suggests strongly that, although T_n is not determined by impurities, it is affected by interactions between the liquid metal droplet and its surroundings. In other words, the nucleation in these cases is still heterogeneous, catalysed by the surface of the droplet, not by impurities. It is thus not clear whether true homogeneous nucleation is ever observed for liquid metals. One possible exception is liquid gallium, which undergoes the largest relative undercooling of any liquid known, nucleating at a temperature half that of its equilibrium freezing point [40].

Perepezko's measurements of T_n, although they may not represent homogeneous nucleation, are nevertheless of considerable interest. His work has shown that when pressure is applied to a simple liquid, the change in nucleation temperature follows that of the freezing temperature. Thus bismuth, which expands on freezing, shows decreases in both T_f and T_n with pressure [41]. There are also interesting results related to the phase selection in strongly undercooled liquids. If a liquid is cooled sufficiently, more than one solid phase can form, and the result may not be that predicted by equilibrium thermodynamics. Perepezko applied the droplet emulsion technique to gallium, achieving undercoolings large enough to permit the formation of five different crystalline phases [42]. He also used a very different method of pulsed laser annealing to form liquid manganese undercooled by 122 K [43]. Many of Perepezko's other experiments apply to crystallization of alloys, a problem that lies outside the scope of this review.

Another important set of measurements has focussed on nucleation of crystallization near the glass transition of the fluid. The driving force for nucleation (the denominator of the exponential in (27)) increases rapidly as a liquid is undercooled, but as the glass transition is approached, the dynamics reflected in the prefactor slows down drastically. The nucleation rate thus passes through a maximum near the glass transition, and in appropriate cases the variation of rate with temperature can be studied. Angell and co-workers examined the temperature–time-transformation (TTT) curves for ice nucleation from LiCl solution, suspended as small drops in an emulsion [44]. The conditions are such that each droplet undergoes multiple nucleation events as its crystallization is monitored by thermal analysis. As predicted, the nucleation rates fall off on either side of the glass transition.

A number of research groups have investigated nucleation of crystals in molten alkali silicates near their glass transitions [14, 16, 45, 46]. Here, the transient as well as steady-state population of nuclei can be monitored. Comparison with predictions of classical theory is made difficult by the large undercoolings and uncertainty about possible temperature dependence of the liquid–solid surface free energy [47].

A different and promising new technique for studying liquid–solid nucleation

involves supersonic nozzle expansions, in which gas streams are cooled as they expand adiabatically. Nibler and co-workers [48] used stimulated Raman scattering to study the crystallization of nitrogen in liquid clusters, while Bartell and Dibble used electron diffraction to examine the freezing of CCl_4 [49] and CH_3CCl_3 [50]. The nucleation rates measured in this type of experiment can be very high: that quoted in [49] was of the order of 10^{23} cm^{-3} s^{-1}. These experiments share the advantage of the emulsion techniques described earlier that the liquid droplets are small enough so that nucleation by impurities can be excluded. In addition, however, the free surface of the droplet in these experiments is better defined than the oxide-covered surface typical of liquid metal in oil emulsions.

4. Beyond classical nucleation theory

4.1. Modifications of the capillarity approximation

The deviations between experiment and classical nucleation theory for the gas–liquid transition described in section 3.1 have stimulated the search for improved theoretical models of nucleation rates. In this section, we discuss some modifications of classical theory, and postpone until sections 5 and 6 newer approaches based on density-functional theory and computer simulation.

There has been a long-standing controversy about the free-energy change associated with forming a critical nucleus, and whether terms in addition to the surface free energy contribution of (13) should be included. Lothe and Pound [51] argued that a cluster has translational and rotational degrees of freedom, and that additional terms in the free energy should be included to take these into account. The result is an increase in nucleation rates by a factor of the order of 10^{17} and, in most cases, a marked worsening of agreement between theory and experiment. Reiss [52] argued that the use of an experimental surface tension within the capillarity approximation already includes most of the effect of fluctuations in the centre of mass and rotation of a liquid-like cluster, and that the Lothe–Pound theory results in an overcounting of these effects. In the Reiss–Katz–Cohen theory [53], an attempt is made to incorporate these two effects consistently, and the result is once again much closer to the original classical theory. A final paper by Pound [54], however, indicates that the question is still not settled to everyone's satisfaction.

Girshick and Chiu suggested a different extension of classical nucleation theory [18]. They used a kinetic approach (resembling that in section 2.1 above) and stressed the role of the extra factor of the supersaturation S in the expression for the nucleation rate. They made one additional change as well, however. They noted that the expression used in classical nucleation theory for the free-energy change to create a cluster of size i from monomer in the vapour at pressure P_e

$$\Delta G_i = \sigma A(i) \tag{29}$$

cannot hold down to size $i = 1$, because there can be no free-energy change in that limit (a cluster of size 1 is already monomer). They therefore suggest a way to make this expression 'self-consistent' by subtracting the contribution at $i = 1$, and take

$$\Delta G_i = \sigma(A(i) - A(1)). \tag{30}$$

This gives the proper limit $\Delta G_1 = 0$, and introduces an additional factor of e^{θ} into the rate, where θ is defined in (15). Questions can be raised about the validity of this *ad hoc* adjustment, however. As has been stressed earlier, classical theory never claims to describe correctly clusters of one or a few atoms, nor does it need to. What is needed is only an estimate of the free-energy change to create a cluster of i^* atoms from monomer, and it is unclear whether (29) or (30) does a better job at this. Equation (30) is a rather arbitrary choice that may empirically improve the fit to experiment.

Another extension of classical nucleation theory was suggested by Dillmann and Meier [55, 56]. It begins with Fisher's phenomenological droplet model [57] for the free energy to create a droplet of size i at pressure P_e

$$\Delta G_i = \kappa(i)\sigma A(i) + \tau k_B T \ln i - k_B T \ln q_0. \tag{31}$$

The second and third terms in this free energy (proportional to ln i and constant) arise from differences between the molecular structure of a free cluster of i molecules and of a group of the same number of particles in the bulk liquid. Classical nucleation theory is recovered by setting q_0 to 1 and τ to 0; the Lothe–Pound model [51] sets $\tau = -4$. The function $\kappa(i)$ goes asymptotically to 1 for large clusters, but corrects for effects of curvature on the surface tension for smaller clusters. Dillmann and Meier assumed the functional form

$$\kappa(i) = 1 + \alpha_1 i^{-1/3} + \alpha_2 i^{-2/3}. \tag{32}$$

The parameters τ and q_0 were then chosen to fit the critical density and pressure of the fluid, while α_1 and α_2 were temperature-dependent quantities selected to fit the saturated vapour pressure P_e and the second virial coefficient. The parameter τ turned out to have a value of 2.2, quite different from that in the Lothe–Pound theory. Agreement with experiment was quite good for substances ranging from nonane to water and the alcohols. It seems surprising that a theory with parameters chosen to fit critical point and low-density gas properties appears so successful at giving free energies of formation of large clusters away from the critical point. The reasons for this success need to be explored further.

The extension of classical nucleation theory to binary mixtures lies outside the scope of this review. It is worth mentioning briefly that Reiss showed in 1950 [58] how two-component systems have critical clusters whose properties can be related to the surface tension of the liquid mixture and to the bulk thermodynamics of the binary system. When the surface tension depends on composition, certain thermodynamic inconsistencies can arise, however, which relate to the proper treatment of surface adsorption [59]. Wilemski has proposed a 'revised classical theory' that reduces to ordinary classical nucleation for a single-component system but that is consistent thermodynamically [60]. It allows the composition of a 'surface layer' in a cluster to vary independently of the bulk composition. As for all generalizations of classical theory, the question of the applicability of macroscopic concepts to small clusters remains an open one.

4.2. Kinetic approaches

The generalizations of classical nucleation presented in section 4.1 were based on estimates of forward rates for cluster reactions (found from gas kinetic theory) and

equilibrium constants for these reactions (involving free energies of formation of clusters). It is equally possible to develop theories for both the forward and backward rate constants and not discuss free energies at all. In principle, this could give a way to calculate nucleation rates directly from the interaction potential, without direct reference to measured surface tensions, which are macroscopic properties. A number of approaches in this direction have recently been described. As we shall see, the sensitivity of nucleation rates to parameters in the theories make such true first-principles approaches almost impossible, especially given uncertainties about interaction potentials for substances studied experimentally. As a result, comparison with experimental data requires fitting either the surface tension or the nucleation rates themselves, limiting the ability of experiment to test theory.

One interesting contribution in this direction was proposed by Nowakowski and Ruckenstein [61]. They calculated rates of loss of particles from clusters by using a diffusion equation in energy space to describe the process by which a particle at the surface of a cluster gains enough energy to escape. In a second paper [62] they employed a full Fokker–Planck equation for motion on the surface of a cluster. The two parameters in the interaction potential they used were fit to give the correct density of the liquid and the proper surface tension (from the Kelvin equation) for large spherical clusters. The latter condition ensures that the theory will reduce to classical nucleation theory for large clusters (small supersaturations). The results showed deviations of the critical supersaturation from classical theory, with the more realistic Fokker–Planck theory showing smaller deviations than the simpler earlier approach.

Hale [65a] has proposed a scaling model for nucleation in which, for fixed nucleation rate, the supersaturation varies with temperature as

$$\ln S_{\alpha} = 0.53\{\Omega(T_c/T - 1)\}^{3/2}.$$

This equation can be derived from classical nucleation theory by making the additional assumptions that the pre-exponential factor varies only slowly with temperature and that the surface tension varies linearly with temperature, vanishing at the critical point. In this case, the parameter Ω is the surface entropy per particle, and should have a nearly universal value. Although the only derivation of this equation is from classical nucleation theory, it seems to work reasonably well even in cases where classical theory breaks down. The reasons for this are not known.

Kobraei and Anderson [63, 64] did not use a kinetic approach (calculating backward rate constants) but tried to avoid using the surface tension in evaluating free energies of small clusters. Instead, they carried out an approximate evaluation of the partition function. Their final result depends on a temperature-dependent effective range parameter, however, which was fit to experimental nucleation rates. There is no way to test the correctness of the assumptions in this theory, as a result.

Wilcox and Bauer [65] extended the usual kinetic model for addition and loss of particles by clusters to include separate steps where excited clusters (formed by addition to particles) are relaxed by collisions with monomer or background gas. Clusters can also be excited by such collisions. This doubles the number of rare constants, and many assumptions need to be made before nucleation rates are calculated. Again, reasonable choices of parameters led to fits to experimental data, but the theory was not really tested.

5. Density-functional methods

5.1. Gas–liquid transition

The methods of calculating cluster free energies described in section 4 were largely macroscopic, relying on the measured surface free energies of liquids and solids. Those to be considered in section 6 are fully microscopic, beginning only with an assumed interaction potential. In this section, we discuss an interesting intermediate approach, one which is macroscopic in using an average density rather than atomic coordinates, but which nonetheless retains effects characteristic of molecular distance scales.

The starting point of the density-functional approach to statistical mechanics is the rigorous proof that there exists a free-energy functional of the average density whose minima give the thermodynamically stable densities at any given temperature and pressure [66]. It is convenient in the case of phase transitions to work in the grand ensemble, in which particle numbers fluctuate. The free-energy functional $\Omega_V[\rho(r)]$ then satisfies the conditions

$$\delta\Omega_V[\rho(r)]/\delta\rho(r) = 0 \qquad \text{at } \rho(r) = \rho_{eq}(r) \tag{33}$$

and

$$\Omega_V[\rho_{eq}(r)] = -pV \tag{34}$$

where $\rho_{eq}(r)$ is the equilibrium average density, p is the pressure, and V the volume. Density-functional methods are particularly useful in studying inhomogeneous fluids, in which the density varies in space because free interfaces or walls are present [67].

Although density-functional methods are in principle exact, real calculations require approximations. One of the first and most important of these is the Cahn–Hilliard theory of interfaces and nucleation, which was first applied to binary sysems but which is easily rewritten for the single-component gas–liquid transition considered here. Suppose first that the free energy were a purely local functional of the density. In this case it could be written as

$$\Omega_{V,\,\mathrm{loc}}[\rho] = \int \mathrm{d}r\ [f_u(\rho(r)) - \mu\rho(r)] \tag{35}$$

where f_u is the Helmholtz free energy per unit volume for a system at (uniform) density ρ, and we have taken advantage of the Legendre transform relation between the Helmholtz free energy and the grand potential, with μ the chemical potential. In mean-field theory, $f_u(\rho) - \mu\rho$ will have a double minimum at temperatures below the critical point, giving stable gas and liquid phases (figure 1). This local functional will not give a reasonable interface in an inhomogeneous system, however. If boundary conditions are assigned so that the density on one side approaches that of the liquid and on the other that of the vapour, the lowest free energy will clearly be achieved by taking an infinitely sharp interface. The free-energy functional must therefore be non-local, in order to incorporate the cost in free energy associated with spatial variation of the density.

One way to do this was that adopted by Cahn and Hilliard [68], who added a square-gradient term to the functional:

$$\Omega_V[\rho] = \int \mathrm{d}r\ \left[f_u(\rho(r)) - \mu\rho(r) + K(\nabla\rho(r))^2\right] \tag{36}$$

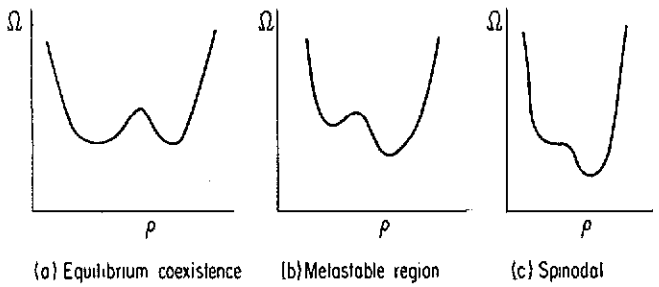

Figure 1. The free energy Ω for a uniform fluid of density ρ, calculated in mean-field theory. Note that the free-energy minimum at lower density loses even local stability at the spinodal. In the metastable region, an activated process is necessary to form the new, higher-density phase.

The coefficient K can depend on density as well; because K is positive, this last term favours a broad interface, where the uniform term favours a narrow one. Taking the functional derivative of Ω_V leads to a differential equation satisfied by the density profile through a planar interface; the solution $\rho(z)$ allows the surface tension to be calculated through the relation

$$\Delta\Omega = \sigma A \tag{37}$$

where $\Delta\Omega$ is the difference in grand potential between the two-phase system with a planar interface of area A and that of pure liquid or vapour at coexistence.

Cahn and Hilliard also used this free-energy functional to study nucleation [69]. In a supersaturated vapour, there is no longer a stable solution of the variational equation that includes both vapour and liquid: the liquid phase is stable, the vapour phase is metastable, and a planar interface would be unstable toward growth of the liquid phase. The density profile of the critical nucleus $\rho(r)$ is, however, a saddle point in 'function space' between vapour and liquid, so the same condition $\delta\Omega_V/\delta\rho = 0$ applies in this case. This leads to a radial differential equation for the density profile

$$\partial f_u/\partial\rho - 2K\ \nabla^2\rho - (\partial K/\partial\rho)(\nabla\rho)^2 = \mu. \tag{38}$$

For small supersaturations S, solutions of this equation give radial density profiles and free energies close to those expected from classical nucleation theory. The behaviour is quite different, however, on approach to the spinodal, the point at which the vapour changes from being metastable to unstable. Near the spinodal, the density change in the critical nucleus becomes small in magnitude but large in extent: the radius of the nucleus, which shrinks initially with increasing supersaturation, eventually reaches a minimum and begins to grow. In addition, the free-energy barrier to nucleation vanishes at the spinodal. This behaviour, which is at the heart of the distinction between a metastable and an unstable phase, is a significant advantage of density-functional methods over classical nucleation theory, in which the nucleation barrier remains finite at the spinodal. Nucleation near the spinodal has been studied further by Klein, who predicts the critical nuclei in this limit to be highly ramified, fractal structures [70].

The square-gradient approximation will be useful if the free energy is only slightly non-local, since it corresponds to a truncated expansion in gradients of the density.

For a sharply varying interface, this will not be correct. Subsequent studies of gas–liquid nucleation by Oxtoby and co-workers [71, 72] avoided this approximation by working with full non-local functionals. This work adopted the philosophy of van der Waals in taking the interaction potential between molecules to be the sum of a harsh repulsive part (modeled with hard spheres) and an attractive tail $\phi_{att}(r)$. The former was assumed to be short enough in range to be treated with a local free-energy functional (the known free energy f_h of a fluid of hard spheres), while the latter was included using perturbation theory. The free-energy functional then has the form

$$\Omega_V[\rho] = \int \mathrm{d}\boldsymbol{r}\ [f_h(\rho(\boldsymbol{r})) - \mu\rho(\boldsymbol{r})] + \frac{1}{2}\int\int \mathrm{d}\boldsymbol{r}\ \mathrm{d}\boldsymbol{r}'\ \phi_{att}(|\boldsymbol{r}-\boldsymbol{r}'|)\rho(\boldsymbol{r})\rho(\boldsymbol{r}'). \quad (39)$$

The functional derivative of this equation gives not a differential equation but an integral equation for the critical density profile:

$$\mu_h(\rho(\boldsymbol{r})) = \mu - \int \mathrm{d}\boldsymbol{r}'\ \rho(\boldsymbol{r}')\phi_{att}(|\boldsymbol{r}-\boldsymbol{r}'|) \quad (40)$$

where $\mu_h(\rho) = \mathrm{d}f_h(\rho)/\mathrm{d}\rho$ is the hard-sphere chemical potential. This equation can be solved by iteration: a density profile is guessed and substituted into the right-hand side and the integral is evaluated numerically. The non-linear function on the left is then inverted to find the new density profile. Because the critical nucleus is a saddle point rather than a stable minimum, the iteration process will eventually diverge toward uniform vapour or uniform liquid, but the saddle point can be located numerically and the free-energy barrier $\Delta\Omega^*$ to nucleation evaluated. In [71] and [72] the nucleation rate was then taken to be

$$J = J_0\ \exp(-\Delta\Omega^*/k_BT) \quad (41)$$

with the same pre-exponential J_0 used as in classical nucleation theory.

In [71], Oxtoby and Evans employed a Yukawa attractive interaction

$$\phi_{att}(r) = -\alpha\lambda^3\ \exp(-\lambda r)/4\pi\lambda r. \quad (42)$$

Although this is not highly accurate for real molecules, the range parameter λ plays an interesting role. When λd was set to 1 (where d is the hard-sphere diameter), very large deviations from classical nucleation theory were predictred (19 orders of magnitude). These are well outside the typical experimental range. An increase in λd to only 1.5 brought the non-classical theory close to classical theory, however (figure 2). For real substances, the value of λd can be estimated from the temperature dependence of the surface tension, giving results in the range of 1.5 to 2, and suggesting that the deviations between classical and non-classical nucleation theories may not be that large in the temperature range studied. The success of classical nucleation theory for the gas–liquid transition is thus an accident of the typical range of attractive potentials. If attractive forces were only slightly longer ranged, classical theory would fail drastically.

A more quantitative attempt to compare with experimental data was carried out in [72], in which a Lennard-Jones potential was used. It was divided into a (temperature-dependent) effective hard-sphere diameter and a long-range attractive part using hard-sphere perturbation theory. Density-functional theory can calculate surface free

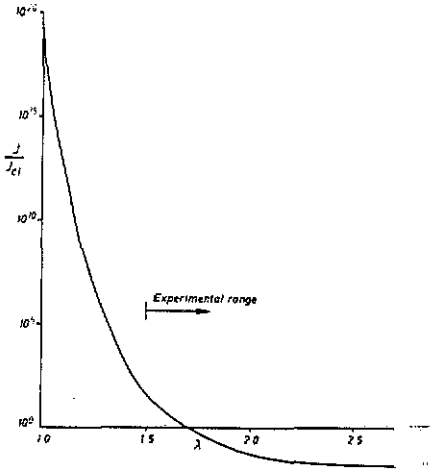

Figure 2. The effect of the (inverse) range of the attractive potential, λ, on the ratio of non-classical to classical nucleation rates. From [71].

energies reasonably accurately (to within 10–20%). Because of the extraordinary sensitivity of nucleation rates to σ, however, the procedure used in [72] was to calculate only the ratio of classical to non-classical nucleation rates, J_{cl}/J_{ncl}, as a function of supersaturation and temperature and to compare it with the result obtained from experiment [31]. The results were revealing: both experiment and theory showed linear plots when ln J_{ncl} was plotted against ln J_{cl} (indicating that the dependence on supersaturation predicted by classical theory is correct). On the other hand, the ratio J_{cl}/J_{ncl} at fixed rate J_{cl} depends strongly on temperature, demonstrating a significant shortcoming of classical theory. The behaviour predicted by the density-functional theory (figure 3) is the same as that observed for nonane and the alcohols. Density-functional theory thus includes crucial non-classical effects associated with the small size of critical nuclei.

In both [71] and [72], bubble nucleation was also studied (cavitation of liquids under negative pressure). In this case, much larger quantitative deviations between J_{cl} and J_{ncl} were predicted: the latter were typically 17 orders of magnitude larger than the former using the Lennard-Jones potential, as a result of the fact that the critical bubble is smaller than the critical droplet at the same temperature. The conclusion is that the tensile strength of liquids (the negative pressure they can sustain before breaking via nucleation) is significantly smaller than that predicted by classical theory. In fact, measured tensile strengths often are smaller than classical predictions [25]. Part of this may be due to heterogeneous nucleation on impurities in the liquid, however.

Zeng and Oxtoby [73] extended the density-functional approach to nucleation of binary vapours, and related the predictions to the thermodynamically consistent, revised classical theory of Wilemski.

The work described so far focussed on the free-energy barrier to nucleation, $\Delta\Omega^*$, and simply adopted the classical pre-exponential rate factor. A more complete theory would calculate the dynamics through the saddle point for the continuum density, using a diffusion equation in function space. Such an approach has been proposed by Langer and Turski [74], who showed that the pre-exponential J_0 is the product of a statistical term (related to the phase-space volume near the saddle point) and a dynamical term (related to the rate of growth of the droplet radius with time due to impingement of gas-phase molecules). Calculation of these two terms for a realistic

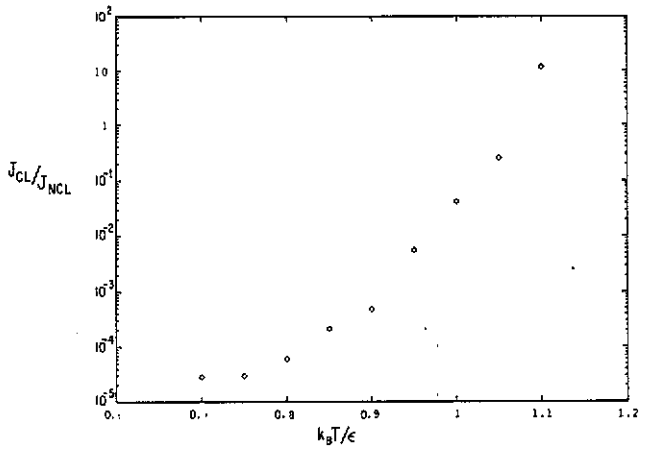

Figure 3. The temperature dependence of the ratio of classical to non-classical nucleation rates for a Lennard-Jones fluid, under conditions where the classical rate is 1 cm^{-3} s^{-1}. From [72].

free-energy functional, including the characteristic dynamics of low-pressure gases, is a priority for the future.

5.2. Liquid–solid transition

In constrast with the studies of liquid–vapour nucleation just described, only one early density-functional calculation of liquid–solid nucleation has been reported. Density-functional methods have been widely applied to determine equilibrium phase coexistence between liquids and solids in simple fluids and binary mixtures [75], but the nucleation problem (which involves non-periodic spatial inhomogeneities in the density) is more difficult to treat.

Harrowell and Oxtoby [76] used a simple perturbative free-energy functional, in which the free energy of the solid (treated as an inhomogeneous fluid) was expanded to second order in the difference in density relative to uniform liquid. The coefficient of the second-order term is related to the direct correlation function $c(r)$, which in turn is connected through Fourier transforms to the structure factor $S(k)$ of the liquid:

$$\rho_l c(k) = 1 - 1/S(k). \tag{43}$$

The latter can be measured experimentally using x-ray or neutron scattering, simulated on a computer, or predicted theoretically. The density of the crystal nucleus was written in the form

$$\rho(\boldsymbol{r}) = \rho_l \sum_{j=0}^{\infty} \mu_j(r) \exp(\mathrm{i}\boldsymbol{k}_j \cdot \boldsymbol{r}) \tag{44}$$

where the sum is over the reciprocal lattice vectors $\boldsymbol{k}_j$ of the crystal, and the term with $j = 0$ allows the average density to change from liquid to solid. Such a representation of the density is correct for a uniform crystal (for which the $\mu_j(r)$ become constants),

and should be reasonable for a spherical crystalline nucleus. The functions $\mu_j(r)$ were assumed to vary more slowly than the actual crystalline density.

The further assumptions made in [76] were that the dominant contribution to $c(k)$ comes from its first peak, and that the order parameters $\mu_j(r)$ vary slowly enough that non-local terms involving them can be treated within a square-gradient approximation. This led to a set of coupled differential equations for the radial variation of order parameters through the nucleus, which were solved numerically by a shooting method. The results were compared with classical nucleation theory (using the same free-energy functional for self-consistency) and showed significant deviations (figure 4). Predicted critical undercoolings from classical and non-classical theories differed sharply, raising questions about the validity of using nucleation experiments (together with classical theory) to measure liquid–solid surface free energies.

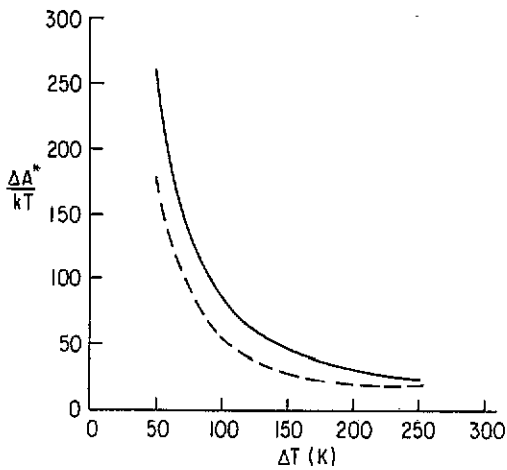

Figure 4. Comparison of the barrier height ΔA^* for nucleation from non-classical theory (solid line) with that from classical theory (dashed line) in a simple model of crystallization of liquid sodium. Nucleation occurs at a rate of 1 cm^{-3} s^{-1} when $\Delta A^*/k_BT$ is of order 70. Significantly different undercoolings ΔT are predicted in this case by the two theories. From [76].

This one nucleation calculation is too approximate to draw strong conclusions, however, Better free-energy functionals have since been developed, and should be applied to the nucleation problem.

6. Computer simulation studies

6.1. Gas–liquid nucleation

Techniques of computer simulation offer the possibility of directly determining the positions of particles during the nucleation of liquids from the vapour. Because of the rarity of nucleation events, it is not possible to simulate nucleation under actual experimental conditions. However, the degree of microscopic detail possible in simulations does allow certain aspects of nucleation theory to be tested directly if appropriate interpretations are made.

In a computer calculation, a prescription must be employed to identify which atoms are in a particular cluster at a given time, because the cluster populations change continuously. One possible definition, proposed by Stillinger [77], takes a cluster to consist of a group of atoms in which each lies within a distance r_c of at least one other atom in the cluster. A second approach, originated by Reiss, Katz

and Cohen [53], defines a cluster as a set of atoms lying within a distance R_c of their centre of mass. With either definition, interactions between clusters allow the statistical mechanics of the system to be calculated exactly in principle; in practice, however, these interactions are often neglected and the results are useful only if there is a plateau over which calculated properties are insensitive to r_c or R_c. If these distances are taken to be too small, no clusters of significant size exist; if they are too large, many 'clusters' actually represent collections of separate subclusters.

Rao, Berne and Kalos [78] used the Stillinger cluster definitions to study nucleation in finite, periodic systems and showed (from classical nucleation theory) that such systems can have a minimum in the free energy for a droplet of definite radius. They then began the simulations with a uniform liquid and expanded the volume, creating a vacuum that was then filled with gas particles as the system approached equilibrium. Both Monte Carlo and molecular dynamics simulations were used, but the latter were less efficient because of the time required to damp out temperature fluctuations as particles evaporated and condensed. The cluster populations were then monitored at equilibrium, and a maximum was found at a point corresponding to the minimum in the free energy; results were insensitive to variation of r_c from 1.7σ to 2.5σ. However, there were too few clusters found in the vicinity of the critical cluster to determine the barrier to nucleation (which would lie between the metastable uniform gas phase and the stable liquid cluster plus gas phase). At low enough temperature, cavitation was also seen.

The second cluster definition, using the distance R_c from the centre of mass, was employed in Monte Carlo calculations of Lee, Barker and Abraham [79]. Note that this condition corresponds to placing the i particles inside a spherical shell of radius R_c. Once again, variation of R_c by 50% changed the free energy per particle by only a small amount at low enough temperatures, although at higher temperatures no plateau value could be established. Such simulations certainly will give reproducible results for the free energy of solid-like clusters, but may not be successful for liquid-like ones in equilibrium with vapour phase at moderate concentration.

Reiss and co-workers have recently taken a significant step toward a true molecular theory of nucleation [80]. Instead of using only the particle number i as identifying parameter of a cluster, they took both i and the cluster volume v, where v is the volume of the sphere about the centre of mass containing the i particles (or, more precisely, bisecting the $(i+1)$st particle [81]). They then showed that the work to create a cluster of i particles in volume v, $W(i, v)$, should have a saddle point as a function of its two variables, and this point can be located by computer simulation. The height of the nucleation barrier can then be rigorously related to the free energy of a system at the saddle point. A key aspect of their approach is that account is taken of interaction with the surrounding vapour; establishing the volume v creates excluded volume that affects the free energy of the entire system. The choice of the volume v is then no longer an artificial constraint but, in their words, 'a procedural device for organizing the counting' of configurations in the partition function. Further results from this approach will be of great interest.

6.2. Liquid–solid nucleation

In a molecular dynamics simulation, the temperature of a liquid can be lowered rapidly by various techniques, the most straightforward of which is to periodically reduce the velocities by a factor, or even to set the velocities to zero. After such a drastic quench, time must be allowed for the system to reach equilibrium at a new

temperature, as potential energy is once again converted into kinetic energy. After a liquid is quenched to a temperature well below its equilibrium freezing point, a glass can form in which particle diffusion vanishes and the system remains amorphous, or a crystal can nucleate and grow. The first observation of crystal nucleation on the computer (in a Lennard-Jones fluid) was due to Mandell *et al* [82], and since that time many systems have been studied. For example, it was shown that relatively modest changes in the potential can reproducibly alter the crystal phase formed from BCC to FCC [83]. The 'moment' at which nucleation occurs can be estimated by randomizing the particle velocities and seeing whether a crystal still forms; if it does, the barrier to nucleation has presumably been crossed.

A major question about this work is whether the periodic boundary conditions affect the nucleation. Earlier work argued that they did not, because the orientation of the crystallite that formed was not directly related to the orientation of the periodic simulation cell. A more definitive answer was provided by the work of Honeycutt and Andersen [84]. If periodic boundary conditions are irrelevent, the nucleation rate should be proportional to the size of the system (as in real experimental situations). What was seen, however, was that the simulated nucleation rate continued to decrease at least out to 1500 Lennard-Jones particles. This shows that nucleation is highly sensitive to the presence of periodic images in neighbouring cells, and calls into question many of the earlier results. A further calculation [85] used 15 000 and then 10^6 particles, and represents one of the largest simulations ever performed. This calculation employed Voronoi polyhedra to obtain precise information about atomic surroundings during nucleation. The results suggested that by 15 000 particles the effects of system size dependence had disappeared, but that the million-particle system was necessary to exhibit the full diversity in nucleation behaviour of a macroscopic system. The size of a critical nucleus under the conditions studied was 10 to 20 particles; for larger critical nuclei (smaller undercoolings) even larger simulations would be required.

A very interesting recent paper [86] studied the height of the free-energy barrier to crystal nucleation for a system of soft repulsive spheres (r^{-12} potential). This approach began by noting that bond orientational order parameters allow one to distinguish liquid from crystal, and different crystal structures from one another. One such parameter, called Q_6, is almost the same for the FCC, HCP and BCC lattices, and was taken as the 'coordinate' joining liquid and solid. The authors used the technique of umbrella sampling to bias the Monte Carlo simulation toward states of high free-energy between uniform liquid and crystal (an unbiased simulation would be overwhelmingly dominated by the regions of lowest free energy). In this way, they were able to extract the variation of free energy with crystallization coordinate Q_6 and measure the height of the barrier. They stressed some important caveats regarding the small size of the systems studied, but nonetheless drew some interesting conclusions. They argued in particular that the BCC crystal forms more easily, not because of a larger thermodynamic driving force, but because the barrier to its nucleation is low. There is no such easy path connecting the liquid to an FCC crystal. The first results from this new technique open up new prospects for the study of crystal nucleation from the melt.

7. Conclusion

Nucleation rates are extraordinarily sensitive to small changes in conditions:

temperature, pressure, impurities, interaction potentials. Although this fact makes the first-principles calculation of nucleation rates quite difficult, it also means that nucleation experiments provide a very sensitive probe of microscopic events. By achieving greater understanding of and control over nucleation rates, we can change the course of first-order phase transitions and perhaps create materials with new and useful properties. Recent advances in the study of nucleation are pointing in the right direction, but much remains to be accomplished.

Acknowledgments

This work was supported by the National Science Foundation through grant CHE 9123172 and through the NSF Materials Research Laboratory at the University of Chicago.

References

[1] Boettinger W J and Perepezko J H 1985 *Rapidly Solidified Crystalline Alloys* ed S K Das, B H Kear and C M Adam (Warrendale, PA: TMS-AIME)
[2] Wagner P E and Vali G (eds) 1988 *Atmospheric Aerosols and Nucleation* (Berlin: Springer)
[3] Toner M, Cravalho E G and Karel M 1990 *J. Appl. Phys.* **67** 1582
[4] Katz J L and Wiedersich H 1977 *J. Colloid Interface Sci.* **61** 351
[5] Oxtoby D W 1988 *Adv. Chem. Phys.* **70** 263
[6] Oxtoby D W 1992 *Fundamentals of Inhomogeneous Fluids* ed D Henderson (New York: Marcel Dekker) ch 10
[7] See, however,
Strey R, Schmeling T and Wagner P E 1986 *J. Chem. Phys.* **85** 6192
[8] Shi G, Seinfeld J H and Okuyama K 1990 *Phys. Rev.* A **41** 2101
[9] Shi G and Seinfeld J H 1991 *J. Mater. Res.* **6** 2091
[10] Schneidman V A 1991 *Phys. Rev.* A **44** 2609
[11] Schneidman V A 1991 *Phys. Rev.* A **44** 8441
[12] Shi G, Seinfeld J H and Okuyama K 1991 *Phys. Rev.* A **44** 8443
[13] Kashchiev D, Verdoes D and van Rosmalen G M 1991 *J. Cryst. Growth* **110** 373
[14] James P F 1985 *J. Non-Cryst. Solids* **73** 517
[15] Kelton K F, Greer A L and Thompson C V 1983 *J. Chem. Phys.* **79** 6261
[16] Kalinina A M, Filipovich V N and Fokin V M 1980 *J. Non-Cryst. Solids* **38 & 39** 723
[17] Kelton K F and Greer A L 1988 *Phys. Rev.* B **38** 10 089
[18] Girshick S L and Chiu C-P 1990 *J. Chem. Phys.* **93** 1273
Girshick S L 1991 *J. Chem. Phys.* **94** 826
[19] See, for example,
Katz J L 1970 *J. Chem. Phys.* **52** 4733
[20] Courtney W G 1961 *J. Chem. Phys.* **35** 2249
[21] Blander M and Katz J L 1972 *J. Stat. Phys.* **4** 55
[22] Swope W C and Andersen H C 1990 *Phys. Rev.* B **41** 7042
[23] Katz J L and Spaepen F 1978 *Phil. Mag.* B **37** 137
[24] Turnbull D and Fisher J C 1949 *J. Chem. Phys.* **17** 71
[25] Hirth J P and Pound G M 1963 *Condensation and Evaporation: Nucleation and Growth Kinetics* (London: Pergamon)
[26] El-Shall M S, Bahta A, Rabeony H and Reiss H 1987 *J. Chem. Phys.* **87** 1329
[27] Reiss H, Rabeony H, El-Shall M S and Bahta A 1987 *J. Chem. Phys.* **87** 1315
[28] Wright D, Caldwell R and El-Shall M S 1991 *Chem. Phys. Lett.* **176** 46
[29] Martens J, Uchtmann H and Hensel F 1987 *J. Phys. Chem.* **91** 2489
[30] Katz J L 1970 *J. Chem. Phys.* **52** 4733
[31] Hung C-H, Krasnopoler M J and Katz J L 1989 *J. Chem. Phys.* **90** 1856

[32] Schmitt J L, Zalabsky R A and Adams G W 1983 *J. Chem. Phys.* **79** 4496
[33] Adams G W, Schmitt J L and Zalabsky R A 1984 *J. Chem. Phys.* **81** 5074
[34] Wagner P E and Strey R 1984 *J. Chem. Phys.* **80** 5266
[35] Strey R, Wagner P E and Schmeling T 1986 *J. Chem. Phys.* **84** 2325
[36] Peters F and Paikert B 1989 *J. Chem. Phys.* **91** 5672
[37] Sharaf M A and Dobbins R A 1982 *J. Chem. Phys.* **77** 1982
[38] Turnbull D 1950 *J. Appl. Phys.* **21** 1022
[39] Suck J-B, Perepezko J H, Anderson I E and Angell C A 1981 *Phys. Rev. Lett.* **47** 424
[40] Bosio L and Windsor C G 1975 *Phys. Rev. Lett.* **35** 1652
[41] Yoon W, Paik J S, LaCourt D and Perepezko J H 1986 *J. Appl. Phys.* **60** 3489
[42] Perepezko J H and Anderson I E 1980 *Synthesis and Properties of Metastable Phases* ed E S Machlin and T J Rowland (Warrendale, PA: TMS-AIME)
[43] Follstaedt D M, Peercy P S and Perepezko J H 1986 *Appl. Phys. Lett.* **48** 338
[44] MacFarlane D R, Kadiyala R K and Angell C A 1983 *J. Chem. Phys.* **79** 3921
[45] Burnett D G and Douglas R W 1971 *Phys. Chem. Glasses* **12** 117
[46] Klein L C, Handwerker C A and Uhlmann D R 1977 *J. Cryst. Growth* **42** 47
[47] Weinberg M C and Zanotto E D 1989 *J. Non-Cryst. Solids* **108** 99
[48] Beck R D, Hineman M F and Nibler J W 1990 *J. Chem. Phys.* **92** 7068
[49] Bartell L A and Dibble T S 1991 *J. Phys. Chem.* **95** 1159
[50] Dibble T S and Bartell L S 1992 *Preprint*
[51] Lothe J and Pound G M 1962 *J. Chem. Phys.* **36** 2080
[52] Reiss H 1970 *J. Stat. Phys.* **2** 83
[53] Reiss H, Katz J L and Cohen E R 1968 *J. Chem. Phys.* **48** 5553
[54] Ruth V, Hirth J P and Pound G M 1988 *J. Chem. Phys.* **88** 7079
[55] Dillmann A and Meier G E A 1989 *Chem. Phys. Lett.* **160** 71
[56] Dillmann A and Meier G E A 1991 *J. Chem. Phys.* **94** 3872
[57] Fisher M E 1967 *Physics* **3** 255
[58] Reiss H 1950 *J. Chem. Phys.* **18** 840
[59] Renninger R G, Hiller F C and Bone R C 1981 *J. Chem. Phys.* **75** 1584
[60] Wilemski G 1987 *J. Phys. Chem.* **91** 2492
[61] Nowakowski B and Ruckenstein E 1991 *J. Chem. Phys.* **94** 1397
[62] Nowakowski B and Ruckenstein E 1991 *J. Chem. Phys.* **94** 8487
[63] Kobraei H R and Anderson B R 1991 *J. Chem. Phys.* **94** 590
[64] Kobraei H R and Anderson B R 1991 *J. Chem. Phys.* **95** 8398
[65] Wilcox C F and Bauer S H 1991 *J. Chem. Phys.* **94** 8302
[65a] Hale B 1986 *Phys. Rev.* A **33** 4156
[66] Evans R 1979 *Adv. Phys.* **28** 143
[67] Henderson D (ed) 1992 *Fundamentals of Inhomogeneous Fluids* (New York: Marcel Dekker)
[68] Cahn J W and Hilliard J E 1958 *J. Chem. Phys.* **28** 258
[69] Cahn J W and Hilliard J E 1958 *J. Chem. Phys.* **31** 688
[70] Unger C and Klein W 1984 *Phys. Rev.* B **29** 2698
[71] Oxtoby D W and Evans R 1988 *J. Chem. Phys.* **89** 7521
[72] Zeng X C and Oxtoby D W 1991 *J. Chem. Phys.* **94** 4472
[73] Zeng X C and Oxtoby D W 1991 *J. Chem. Phys.* **95** 5940
[74] Langer J S and Turski L A 1973 *Phys. Rev.* A **8** 3230
[75] Haymet A D J 1987 *Science* **236** 1076
[76] Harrowell P and Oxtoby D W 1984 *J. Chem. Phys.* **80** 1639
[77] Stillinger F H 1963 *J. Chem. Phys.* **38** 1486
[78] Rao M, Berne B J and Kalos M H 1978 *J. Chem. Phys.* **68** 1325
[79] Lee J K, Barker J A and Abraham F F 1973 *J. Chem. Phys.* **58** 3166
[80] Reiss H, Tabazadeh A and Talbot J 1990 *J. Chem. Phys.* **92** 1266
[81] Ellerby H M, Weakliem C L and Reiss H 1991 *J. Chem. Phys.* **95** 9209
[81] Mandell M J, McTague J P and Rahman A 1976 *J. Chem. Phys.* **64** 3699
[82] Hsu C S and Rahman A 1979 *J. Chem. Phys.* **71** 4974
[84] Honeycutt J D and Andersen H C 1986 *J. Phys. Chem.* **90** 1585
[85] Swope W C and Andersen H C 1990 *Phys. Rev.* B **41** 7042
[86] van Duijneveldt J S and Frenkel D 1992 *J. Chem. Phys.* **96** 4655